

Interplay of Correlation and Relativistic Effects in Correlated Calculations on Transition-Metal Complexes: The $(\text{Cu}_2\text{O}_2)^{2+}$ Core Revisited

Dimitrios G. Liakos and Frank Neese*

Lehrstuhl für Theoretische Chemie, Universität Bonn, Wegelerstrasse 12, D-53115 Bonn, Germany

S Supporting Information

ABSTRACT: Owing to the availability of large-scale computing facilities and the development of efficient new algorithms, wave function-based ab initio calculations are becoming more common in bioinorganic chemistry. In principle they offer a systematic route toward high accuracy. However, these calculations are by no means trivial. In this contribution we address some pertinent points through a systematic theoretical study for the equilibrium between the peroxo- and bis-(μ -oxo) isomers of the $[\{\text{Cu}(\text{C}_2\text{H}_8\text{N}_2)\}_2\text{O}_2]^{2+}$ complex. While this system is often regarded as a prototypical multireference case, we treat it with the single reference local-pair natural orbital coupled cluster method and reiterate that the multireference character in this system is very limited. A set of intermediate structures, for the interconversion between the two isomers, is calculated through a relaxed surface scan thus allowing the calculation of an energetic profile that cleanly connects the bis-(μ -oxo) and side-on peroxo minima on the ground-state potential energy surface. Only at the highest level of theory involving complete basis set extrapolation, triple excitation contributions as well as relativistic and solvent effects, the bis-(μ -oxo) isomer is found to be slightly more stable than the peroxo structure. This is in agreement with the experimental findings. The effects of basis set, triples excitation, relativity, and solvent contribution have all been analyzed in detail. Finally, the ab initio results are compared with density functional calculations using various functionals. It is demonstrated that the largest part of the discrepancies of the results reported in the literature are due to an inconsistent handling of relativistic effects, which are large in both ab initio and density functional theory calculations.

INTRODUCTION

The importance of copper enzymes hardly needs to be emphasized.^{1–14} Within this class, enzymes featuring a binuclear copper active site have received significant attention. Prominent members include catechol oxidase⁸ and tyrosinase^{15,8–10,12} (both catalyzing the oxidation of catecholes to *o*-quinones) and hemocyanin,^{13,16–22} an oxygen transportation protein. The common feature of these enzymes is the $\text{Cu}_2\text{O}_2^{2+}$ core in the active site. Up to six different isomers seem to be accessible for this core. Three of them (Figure 1) have been characterized spectroscopically^{23–26} and crystallographically.^{23,24,26–28} Structure A is the $\mu\text{-}\eta^2\text{:}\eta^2$ -peroxo (side-on) isomer that will be referred to below as P. In this core, the Cu–Cu distance is close to 3.6 Å, and the O–O bond distance is ~ 1.4 Å. Structure B, the bis(μ -oxo) dicopper(III) isomer, is referred to as O below. Here the O–O distance has lengthened to 2.3 Å, which means that the O–O bond has effectively been broken, while the Cu–Cu distance is shortened to ~ 2.8 Å. Structure C, the trans μ -1,2-peroxo species, is less common but was the first motif to be observed crystallographically.²⁷ All of these cores have singlet ground states. In structures A and C copper is in the formal oxidation state of 2+ (d^9 electronic configuration), while in structure B it is 3+. Thus, structures A and C are thought to represent magnetic coupling cases, in which case a closed shell determinant does not provide a good description of the electronic structure, and multireference approaches [or broken symmetry density functional theory, (DFT)] appear to be necessary to obtain reasonable results. Thus, the $(\text{Cu}_2\text{O}_2)^{2+}$ core has

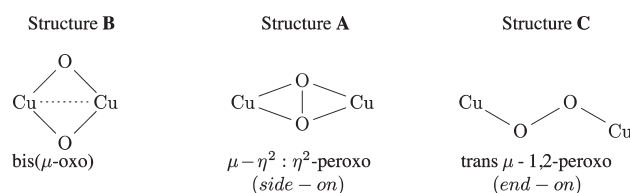


Figure 1. The three most common structures of the $\text{Cu}_2\text{O}_2^{2+}$ core.

become a playground for theoreticians testing different theoretical approaches. A concise review of the literature up to 2009 has been published by Ghermann and Cramer.⁷ Owing to the concept that P requires a multireference treatment, massive multireference calculations using the complete active space self-consistent field/complete active space second-order perturbation theory (CASSCF/CASPT2) and multireference configuration interaction (MRCI) methodologies have been undertaken.^{29–34} However, as will be discussed below, structure A is so strongly coupled that it is outside the magnetic coupling regime, and treatments starting from a closed shell determinant are adequate. Probably the most accurate calculations to date have been performed by Cramer et al.^{29,31} using the CR-CC-(2,3)^{35–37} approach.

It has nevertheless become evident from the many theoretical studies performed on the system that proper theoretical

Received: December 2, 2010

Published: April 20, 2011

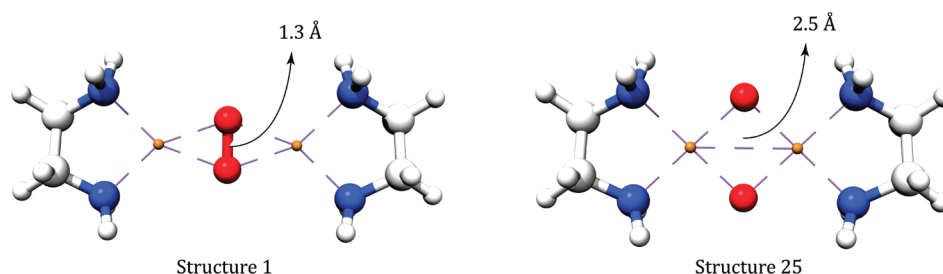


Figure 2. The structure of the first step (left) and the one after step 25 (right).

modeling of the $(\text{Cu}_2\text{O}_2)^{2+}$ core is challenging and that theoretical results with both DFT and wave function-based approaches scatter widely.^{7,33,38–41} The available studies range from treatments of the bare core^{29,34,40–43} up to complexes containing six histidines as terminal ligands.⁴⁴ It became evident that DFT results depend strongly on the specific form of the chosen functional.^{29–32,38,39,44–52} The wave function-based calculations suffer from the fact that small models are not experimentally accessible, and hence comparison of theoretical results for the naked $(\text{Cu}_2\text{O}_2)^{2+}$ core to experiment are not possible. On the other hand, realistic size models are too large to be accurately treated with either single- or multireference wave function methods in conjunction with adequately large basis sets. At the multireference level, the CASSCF method has been used and found to be inadequate due to the lack of dynamic correlation contributions^{53,54} and probably also due to excessive active space requirements. Adding part of the dynamical correlation through perturbation theory in the form of either the CASPT2⁵⁵ or the restricted active space second-order perturbation theory (RASPT2)³³ method can in principle improve the performance,^{29–34} but satisfactory convergence with respect to the size of the reference space is difficult to achieve. In this respect the RASPT2 method, which allows for significantly more active space orbitals, is an important step. However, dictated by the high computational cost, the available correlated ab initio calculations that do include dynamic correlation contributions all featured relatively small double- ζ type basis sets that certainly fall short of coming close to the basis set limit. In addition, they were done on small models with ammonia model ligands. Hence, the theoretical results so far suffer from significant basis set incompleteness problems.

In this work we study the problem using the recently developed local pair natural orbital coupled cluster method.^{56–58} This method can handle realistic models of actual dicopper cores while still employing quadruple- ζ size basis sets and reproducing the parent canonical correlation methods with an accuracy of 0.5 kcal/mol or better.⁵⁸ Therefore, these methods allow for reliably estimating the basis set limit of chemically relevant methods. In doing so, we have investigated a number of additional issues concerning such calculations, namely the interplay of correlation with scalar relativistic and solvent effects. As will be shown below, our most complete calculations are in full agreement with the available experiments. In order to provide a consistent set of calculations, we have also studied a number of DFT functionals and compared them to the ab initio results, with some surprising findings.

Another aspect that differs in our calculations from the literature is the use of a series of structures resulting from a relaxed surface scan along the O—O bond. Previous investigators

have mainly used interpolated structures results (e.g., a rigid scan). As noted by Cramer et al.³¹ such transit paths would be expected to overestimate the isomerization barrier between **P** and **O**.

The simplest type of dicopper core with saturated neutral amine ligands that avoids the complication associated with the use of ammonia (artificial hydrogen bonds, too much coordinative flexibility) contains simply ethylene diamine (*en*) as a capping ligand. Hence, we have chosen to study $[\text{Cu}_2(\text{en})_2(\text{O})_2]^{2+}$ as a representative model. This system is closely related to the one developed and studied by Stack and co-workers.^{1,5,14,25,39,51,59,60} The experimental findings⁵⁹ demonstrate that for this system in dichloromethane solution, **O** should be the predominant species.

COMPUTATIONAL DETAILS

The ORCA suite of programs⁶¹ was used for all calculations. A 25 point relaxed energy surface was constructed along the O—O bond distance between 1.3 and 2.5 Å using the Perdew—Burke—Ernzerhof (PBE)⁶² functional together with Grimme's dispersion correction (Figure 2).⁶³ This way of describing the conversion between the two isomers has the advantage that the energy surface is smooth since the intermediate structures are optimized. Thus, the local maximum connecting the **P** and **O** should be a fairly good guess at the energy of the transition state describing the isomerization between the two forms.

For the wave function-based calculations the local-pair natural orbital coupled cluster (LPNO—CCSD)^{57,58} method was used. The basis sets used were the def2-SVP,⁶⁴ def2-TZVP,^{64,65} def2-TZVPP,^{64,65} and def2-QZVP.⁶⁶ For all calculations, the def2-QZVP/C auxiliary basis set was used for the resolution of identity (RI)^{67,68} approximation that was used throughout. Finally the complete basis set total energies were estimated based on a two-point extrapolation scheme that will be described in detail below.

In the absence of LPNO triples correction, canonical CCSD-(T)^{69,70} calculations were performed in order to estimate triple substitution effects. For these calculations the def2-TZVP basis set was used for copper together with def2-SVP for the remaining atoms. This choice is dictated by computational cost.

For the DFT part of this study, the following functionals were used: B-LYP,^{71,72} B3-LYP,^{71–73} B1-LYP,^{71,72,74} BHandHLYP,^{72,73,75} and B2PLYP.⁷⁶ Motivated by the work of Siegbahn,⁷⁷ dispersion corrections were investigated according to semiempirical method developed by Grimme.⁶³ In these calculations, the def2-TZVP⁶⁵ basis set, together with the corresponding auxiliary basis set, was used.

For all DFT calculations, the restricted Kohn—Sham (RKS) formalism was used. The reason for this choice was that all unrestricted Kohn—Sham calculations gave identical results with

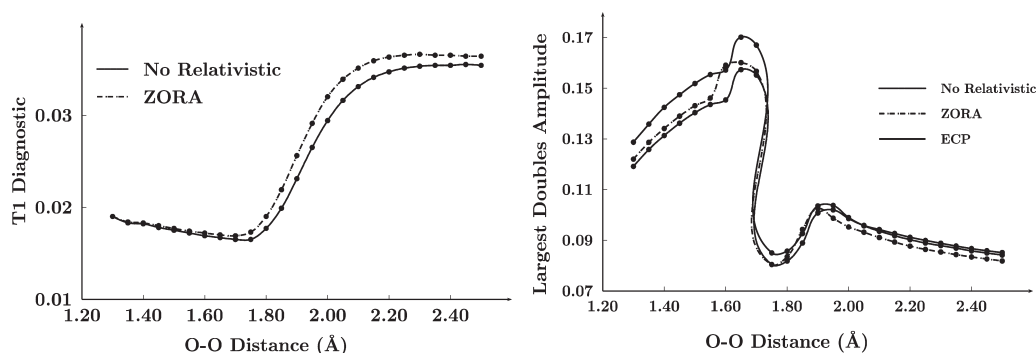


Figure 3. The T_1 diagnostic (left) and the largest doubles contribution in the wave function (right) across the isomerization coordinate, calculated with the LPNO-CCSD method.

the RKS ones (e.g., they maintained symmetry). Broken symmetry calculations were extensively examined. The results showed that up to 20% exact exchange (EEX) (corresponding to the B3LYP functional), no broken symmetry solution was more stable than the RKS one, even in the region of the PES corresponding to **P**. Thus we feel that it is justified to focus on the results of the RKS calculations.

For both wave function- and DFT-based calculations, scalar relativistic effects were treated either explicitly [via the second-order Douglas-Kroll-Hess (DKH) transformation^{78–82} or with the zeroth-order approximation for relativistic effects (ZORA)]^{83,84} or alternatively via effective core potentials (ECPs). In the latter case, the ECP10MWB^{85,86} potential together with the corresponding basis set was used on copper. In the case of ZORA corrected calculations, the all-electron scalar relativistic basis sets described earlier were used.⁸⁷

Solvent effects were treated with the conductor-like screening (COSMO)⁸⁸ approach,^{89–91} as implemented in ORCA.⁹²

WAVE FUNCTION RESULTS

Multireference Character of the $(\text{Cu}_2\text{O}_2)^{2+}$ Core. Since the LPNO-CCSD method chosen for the study is a single reference method, the question concerning the multireference nature of the wave function rises. In the literature, the T_1 diagnostic⁹³ is often employed to judge multireference character. The results in Figure 3 demonstrate that the T_1 diagnostic stays within reasonable bounds over the entire isomerization coordinate and slightly increases upon approaching the **O** isomer. If **P** would be a genuine multireference species (as might be expected from the formal d^9 electron configuration at the two copper(II) ions), the opposite trend would be expected. In fact, as discussed elsewhere,⁹⁴ one should distinguish between the terms ‘multideterminantal’ and ‘multiconfigurational’. The open-shell singlet that dominates the wave function in the case of two weakly antiferromagnetically interacting d^9 systems is multideterminantal but monoconfigurational because a single spatial configuration is involved in both determinants of the open-shell singlet. The term multiconfigurational should be reserved for cases in which different spatial configurations occur in the wave function with large weights.

In agreement with other researchers,³¹ we do not think that the T_1 diagnostic is a good measure of multireference (or multideterminantal) character. In coupled cluster theory, the single excitation amplitudes essentially describe orbital relaxation, and hence, large single contributions are expected when the

Hartree-Fock (HF) orbitals are poor. In the present case, the starting orbitals for **O** appear to be worse than those for **P**, which is a sensible result because the metal ligand covalency is certainly higher for the dicopper(III) species **O** compared to **P** and because HF theory is known to not provide bonds that are far too ionic.

In our opinion, a more valid criterion for multireference character is the largest double excitation amplitudes. For genuine diradicals, the largest amplitude should approach a value of unity in which case the single reference approach as such becomes invalid. Our results are shown in Figure 3. It is indeed observed that the largest doubles amplitudes occur on the **P** side of the isomerization surface. However, even there the largest double excitation amplitude does not exceed a value of 0.17.

Taken together these results imply that the single reference coupled cluster approach is very well suited for describing the $(\text{Cu}_2\text{O}_2)^{2+}$ core over the entire isomerization coordinate connecting the **P** and **O** minima. Obviously, this does not imply that other single reference methods are equally suitable for studying the $(\text{Cu}_2\text{O}_2)^{2+}$ core. Owing to the exponential Ansatz, coupled cluster theory (or its close variants) is certainly the most stable approach and tolerates much larger amounts of multireference character than, say, many body perturbation theory or configuration interaction approaches before breaking down.

Basis Set Limit Estimate. In order to approach the complete basis set (CBS) limit, large scale LPNO-CCSD calculations were performed. The usual practice to achieve this estimate is the use of a two-point extrapolation scheme. As described below, we have used various schemes for this extrapolation. The first combination of basis sets was based on the smallest possible basis set combination and involved the double- ζ /triple- ζ pair def2-SVP/def2-TZVP (referred ExtrapolationS). Second, the much more demanding triple- ζ /quadruple- ζ combination def2-TZVPP and def2-QZVP was used (referred to as ExtrapolationB). The results of this extrapolation are supposed to provide the most accurate results of this work.

The CBS extrapolated energy is estimated^{95,96} according to the formula:

$$E^{(\text{CBS})} = E_{\text{HF}}^{(\text{CBS})} + E_{\text{LPNO-CCSD}}^{(\text{CBS})} \quad (1)$$

Here:

$$E_{\text{HF}}^{(\text{CBS})} = \frac{E_{\text{HF}}^X e^{(-a\sqrt{Y})} - E_{\text{HF}}^Y e^{(-a\sqrt{X})}}{e^{(-a\sqrt{Y})} - e^{(-a\sqrt{X})}} \quad (2)$$

is the estimated CBS HF energy and

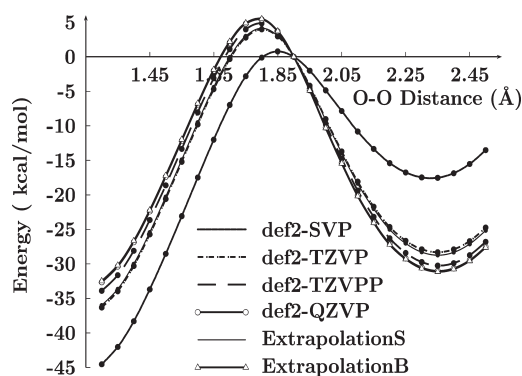


Figure 4. The HF energy calculated across the isomerization coordinate with different basis sets.

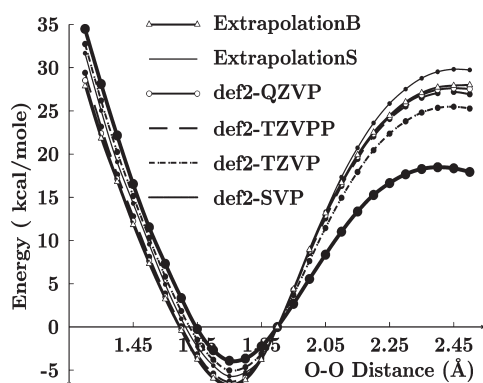


Figure 5. The LPNO-CCSD energy calculated across the interconversion coordinate with different basis sets.

$$E_{\text{LPNO-CCSD}}^{(\text{CBS})} = \frac{X^\beta E_{\text{LPNO-CCSD}}^X - Y^\beta E_{\text{LPNO-CCSD}}^Y}{X^\beta - Y^\beta} \quad (3)$$

the estimated CBS LPNO-CCSD energy. In these equations X and Y are the smaller and larger cardinal numbers of the involved basis sets. We note in passing that the validity of extrapolating with the def2 basis sets has been investigated in ref 97 and was found to be excellent. The values of α and β used were 10.39 and 2.40 for ExtrapolationS and 7.88 and 2.971 for ExtrapolationB.⁹⁷

In Figure 4 the SCF contribution to the total energy (without relativistic corrections and in the gas phase) is presented. It is obvious that the SCF energy converges smoothly to the CBS limit. The SCF energy has practically converged with the def2-QZVP basis set. The largest difference between the CBS energy calculated with ExtrapolationB and the energy calculated with def2-QZVP is 0.1 kcal/mol. The only result that deviates significantly from the CBS limit is, in fact, the uncorrected def2-SVP curve.

In Figure 5 the analogous results are shown for the LPNO-CCSD correlation energy. Fortunately, the correlation energy also appears to converge smoothly, and at the level of the def2-QZVP basis set, the LPNO-CCSD correlation energy has essentially converged to the CBS estimate. The largest deviation between the def2-QZVP and ExtrapolationB results is 0.65 kcal/mol, which is reasonable given that the correlation energy converges much more slowly to the basis set limit than the SCF energy.⁹⁵ However, these deviations are observed at the

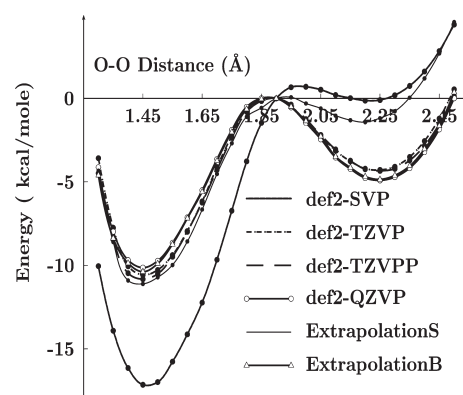


Figure 6. The total energy calculated across the interconversion coordinate with different basis sets.

extreme points of the PES. In the more important regions of the PES, the deviations are again on the order of 0.2 kcal/mol.

Finally in Figure 6 the total PES is plotted as the sum of the previous two terms. The maximum deviation between the def2-QZVP and ExtrapolationB results is 0.48 kcal/mol. Again this occurs at the first and last points of the PES. In the more interesting relevant areas, the deviations are in the order of 0.1 kcal/mol. The deviations in the total energy are smaller than those obtained for the correlation energy alone, since SCF and correlation errors have opposite signs and tend to cancel. Nevertheless, it is concluded that with the def2-QZVP basis set, the PES has essentially converged to the CBS result.

Below, the LPNO-CCSD method is used in conjunction with ExtrapolationB in order to produce the most accurate results achievable with this methodology.

At this point a note concerning an alternative widely used extrapolation scheme is appropriate. In this scheme the CBS correlation energy is estimated on the basis of the MP2 CBS energy. The extrapolated correlation energy is obtained according to the formula:

$$E_{\text{corr}}^{(\text{CBS})} = E_{\text{MP2}}^{(\text{CBS})} + (E_{\text{LPNO-CCSD}}^X - E_{\text{MP2}}^X) \quad (4)$$

Here $E_{\text{corr}}^{(\text{CBS})}$ is the CBS estimation for the correlation energy, calculated according to eq 3 only replacing the LPNO-CCSD energies with MP2 energies. $E_{\text{LPNO-CCSD}}^X$ and E_{MP2}^X are the LPNO-CCSD and MP2 energies calculated with the small basis set. The HF energy is calculated in the same way as before. In the left part of Figure 7 the correlation energy calculated, as described above, using the cc-pVTZ/cc-pVQZ combination of basis sets (referred to as ExtrapolationC), is presented. For comparison in the same figure, the correlation energy calculated with the ExtrapolationB scheme is also plotted.

From the left part of Figure 7, ExtrapolationC strongly stabilizes **P** with respect to **O**. The stabilization of **P** over **O** is as much as 7.1 kcal/mol larger compared to what is obtained with the more rigorous ExtrapolationB scheme. It is obvious that a basis set limit estimate that introduces such a large error is useless for obtaining chemically meaningful results. The reason for this disappointing behavior can be found in the behavior of the MP2 correlation itself energy. In the right part of Figure 7, the correlation energies calculated with the canonical CCSD(T), LPNO-CCSD, and MP2 methods obtained with the same basis set are shown. While the LPNO-CCSD curve closely resembles

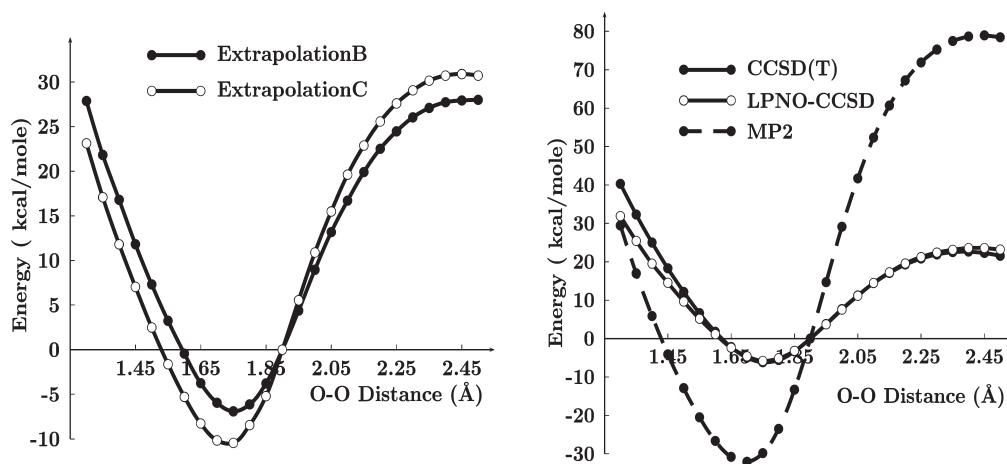


Figure 7. Complete basis set correlation energy estimates using extrapolation schemes ExtrapolationB and ExtrapolationC (left). Relative correlation energies calculated with the CCSD(T), LPNO-CCSD, and MP2 methods (right), (def2-TZVP basis set on for copper and def2-SVP for the remaining atoms).

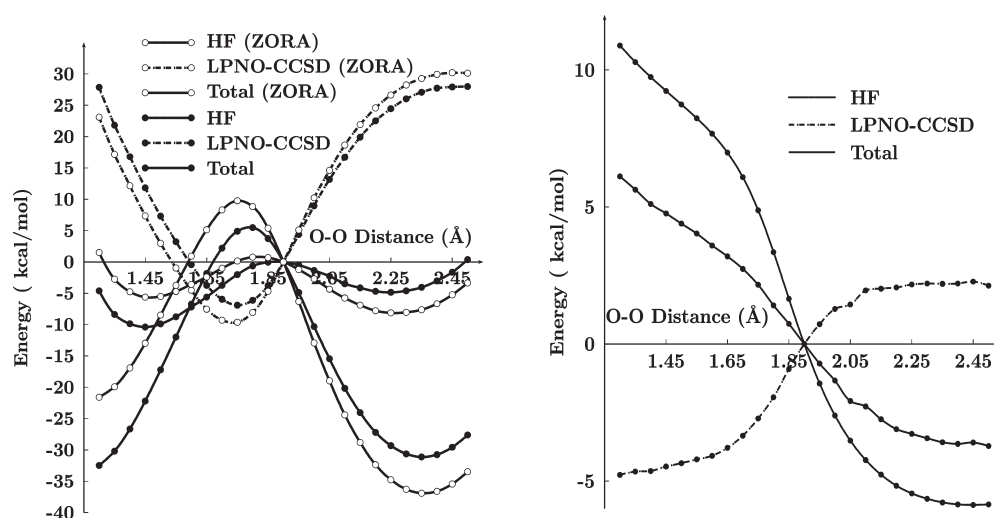


Figure 8. The PES and its components calculated with the LPNO-CCSD method and the ZORA scalar relativistic corrections together with the corresponding nonrelativistic curve (left). The effect of ZORA scalar relativistic corrections to the total energy across the interconversion coordinate (right).

the canonical CCSD(T) one, the MP2 estimate is miserable and dramatically overstabilizes P.

Interplay of Correlation and Relativity. Scalar relativistic effects are usually considered to be of lesser importance in the chemistry of the first transition row.⁹⁸ Nevertheless their importance has already been recognized for some time (e.g., Flock et al., ref 32). In Figure 8 the HF, LPNO-CCSD, and total energies calculated on the basis of ExtrapolationB and the inclusion of scalar relativistic ZORA corrections are shown (gas phase calculations).

The immediate conclusion from Figure 8 is that overall O is stabilized by about 8.4 kcal/mol relative to the P. The second important observation is that the net effect due to relativity arises from the interplay of two competing factors. The relativistic changes to the correlation energy work in favor of P, while the analogous effect on the SCF energy works in favor of O. The net outcome is the sum of these two contributions. Since the effect on the SCF energy is more pronounced, the latter dominates the overall relativistic correction, thus resulting in an overall

stabilization of O. The 8.4 kcal/mol that O gains with respect to P is enough to even change the more stable minimum from P to O. The origin of the large scalar relativistic effects will be investigated below after the DFT results have been presented.

However, before proceeding to analyze the effects of relativity, the effects of perturbative triple excitations will be considered. The canonical CCSD(T) triple corrections obtained in the scalar relativistic and nonrelativistic cases are shown in Figure 9. It is evident that the relativistic corrections are fairly limited and that triple excitations slightly work in favor of O compared to P. Overall, the triples correction favors the O by 2.1 kcal/mol.

Solvent Effects. In this step of the investigation, solvation effects are added to the PES. They have been estimated at the level of the conductor-like screening (COSMO) model using CH₂Cl₂ as a solvent (def2-TZVPP basis set in this section). The difference between gas-phase and solvent results calculated at this level was added to the curve obtained with ExtrapolationB together with the triple substitution effects. The resulting curve is considered the most accurate result of this study and will serve as

a reference for judging the DFT results. In Figure 10, the resulting PES is plotted together with the obtained solvent effect.

From the left part of the figure, the main conclusion is that **O** is more stable than **P** by 4.1 kcal/mol. The estimated transition-state energy is 8.6 kcal/mol higher above **O**. This result would imply facile interconversion of the two isomers with the thermodynamic equilibrium being significantly on the side of **O**. The true transition state must be slightly lower than the saddle point on the PES, as this point is obtained from a constraint optimization.

The additional stabilization of **O** relative to **P** is apparent from the right-hand side of Figure 10. This makes sense as **O** has the constituent atoms in higher formal oxidation states and is more compact than **P**. Both factors are thought to contribute to the extra stabilization of this dication.⁷ The size of the effect is as large as 6 kcal/mol. Thus, the net result that **O** is more stable than **P** is caused by a combination of relativistic and solvent effects.

DENSITY FUNCTIONAL THEORY

Since the largest part of the literature concerning computational studies on dicopper complexes is done with DFT, a detailed study of the factors affecting the outcome of these

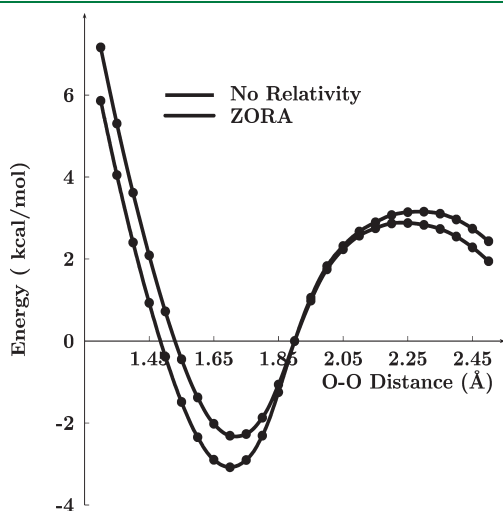


Figure 9. The correlation energy recovered by the perturbative triples correction across the isomerization coordinate calculated without relativistic corrections and after the ZORA correction.

calculations is presented below. The factors studied are the exact exchange contribution in the functional, dispersion forces, scalar relativity, and finally solvent effects.

Effect of Exact Exchange of the Functionals. In order to study the effect of exact exchange (EEX) in the calculated energies, a set of different functionals with varying EEX was used. The functionals were: BLYP^{71,72} (0% EEX), B3LYP^{71–73} (20% EEX), B1LYP^{71,72,74} (25% EEX), BHandHLYP^{72,73,75} (50% EEX), and finally also B2PLYP⁷⁶ (53% EEX). The choice of these functionals was made based on the fact that B3LYP is the most popular functional in current use and that the remaining functionals (except B2PLYP) use the same components and differ mainly in the fraction of EEX. The double hybrid B2PLYP functional also includes a MP2 correction that brings in semilocal correlation effects. The results of our calculations with these functionals in the gas phase and without corrections for relativistic or dispersion forces are presented in Figure 11.

It is obvious that the DFT results depend strongly on the fraction of EEX. In the right-hand part of Figure 11, the energy difference between the **O** and **P** minima is shown. Obviously, the **O** – **P** energy difference is almost linear to the fractional EEX. This was first noted by Rode et al.⁹⁹ and by Cramer et al.^{29,31} and is extended here to the range of 0–50% EEX. A comparison reveals that B3LYP and B1LYP are in best agreement with LPNO–CCSD results (calculated with ExtrapolationB and no relativistic corrections), with B1LYP being slightly preferred. The BLYP functional erroneously predicts the wrong isomer. The B2PLYP functional does not seem to perform well in this application as it gives a much too high energy value for the **O** isomer. In fact it does not even predict a minimum for this species. This must be attributed to the badly failing MP2 component in the B2PLYP energy.

Weak Interactions – D. The correction due to Grimme⁶³ that has been shown to improve the results of DFT calculations^{100,101} was investigated in this part. Parameters are only available for BLYP, B3LYP, and B2PLYP. Hence B1LYP and BHandHLYP were not investigated in this section.

In the left part of Figure 12, the PES calculated with the different functionals after the inclusion of dispersion forces correction is presented. In the right part the effect of these corrections in the functionals is plotted, and one can see there that the addition of dispersion forces correction does not have a significant effect on the relative stability of the two isomers. The

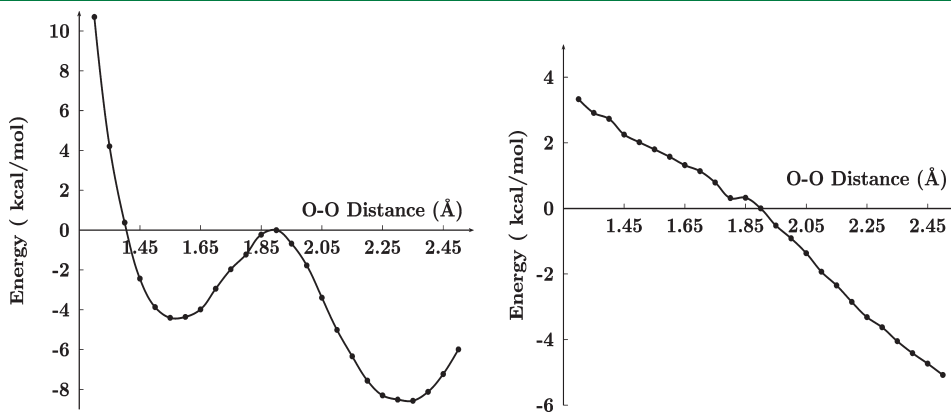


Figure 10. The total energy calculated across the isomerization coordinate estimated at the CBS limit including solvent effects, triples correlation energy, and ZORA relativistic corrections (left). The effect of COSMO on the energy calculated with the LPNO–CCSD method and the def2-TZVPP basis set, including ZORA corrections (right).

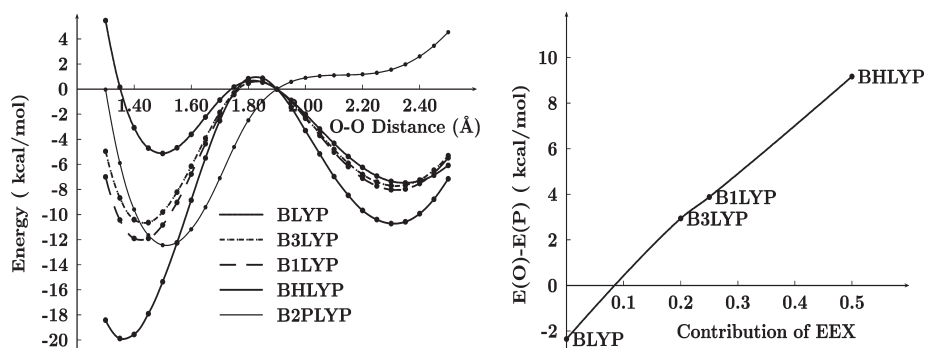


Figure 11. Energy path, following the isomerization coordinate, calculated with various functionals (left). Energy difference $E(O) - E(P)$ plotted against the percentage of EEX contribution in the functional (right).

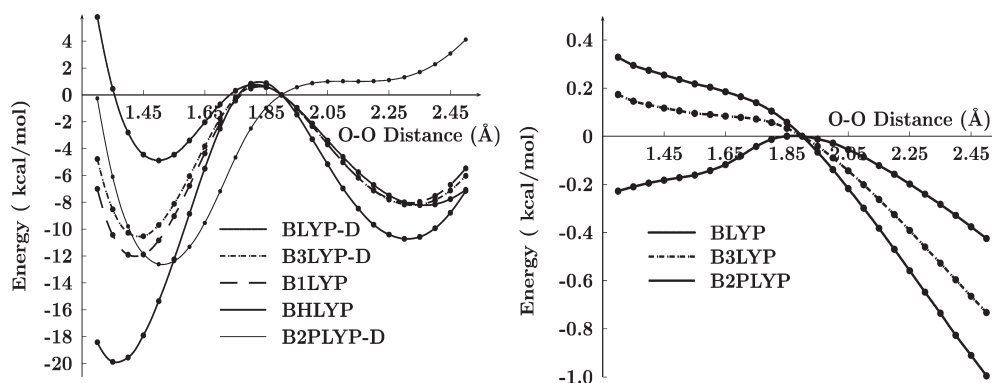


Figure 12. Single point energies calculated across the isomerization coordinate calculated with the correction for dispersion forces (left). Effect of dispersion forces correction (right).

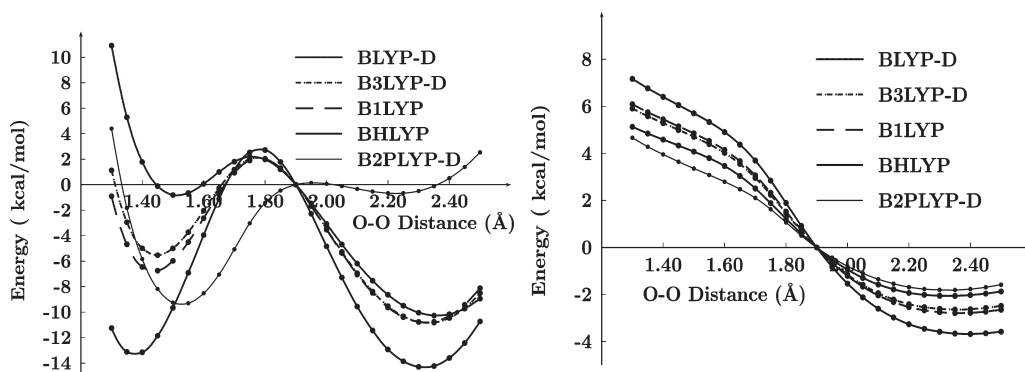


Figure 13. The potential energy using the density functional methods corrected for relativistic effects through ZORA (left part). The effect of ZORA (right part).

quantitative form of the PES remains unchanged, while the largest change in the relative energies is not larger than 1 kcal/mol. However, this result should not be overemphasized, as it has recently been shown that in $(\text{Cu}_2\text{O}_2)^{2+}$ complexes with large ligands, dispersion forces can be significant.⁷⁷

Relativistic Effects. In most of the previous works, relativistic effects were included either implicitly through ECPs or have been ignored. Here an effort is made to systematically investigate the size of these effects. In order to accomplish this, three different approaches were used (the two scalar relativistic corrections, ZORA^{83,84,102} and DKH^{78–82} as well as the ECP

ECP10MWB).^{85,86} In Figure 13 the effect of the ZORA relativistic correction is presented, in Figure 14 the effect of the DKH correction, and finally in Figure 15 the effect of the use of an ECP for Cu.

It is obvious from these figures that the effect of relativity is as pronounced, as in the LPNO–CCSD case, and results in a net stabilization of the **O** isomer. As in the LPNO–CCSD case, relativity switches the order of stability of the two isomers. ZORA and DKH are almost indistinguishable. ECPs lead to a less pronounced relativistic effect. Despite the fact that again **O** is stabilized with respect to **P**, the stabilization is not large enough

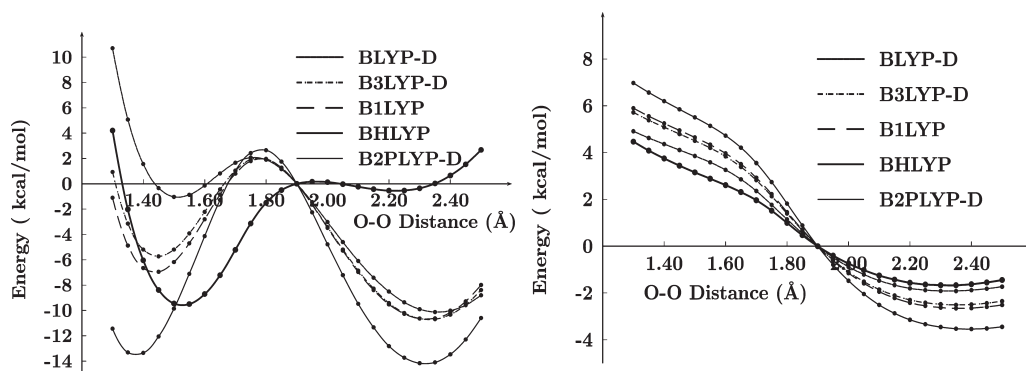


Figure 14. The potential energy using the density functional methods corrected for relativistic effects through DKH (left part). The effect of DKH (right part).

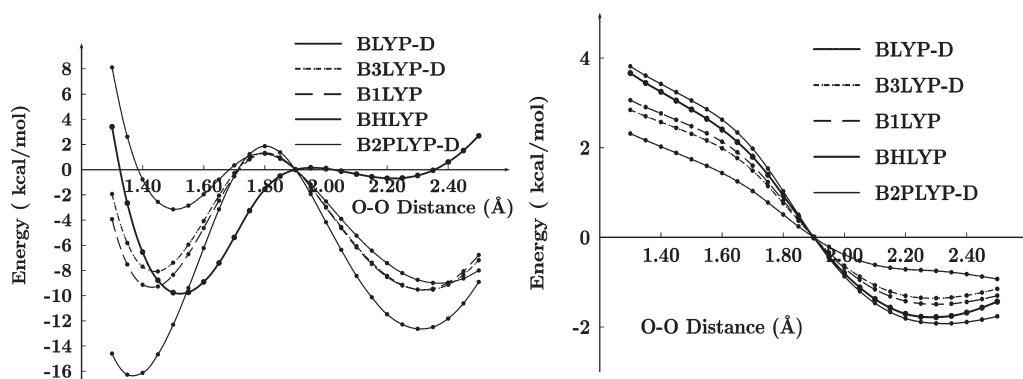


Figure 15. The potential energy using the density functional methods calculated using the quasirelativistic ECP ECP10MWB for copper.

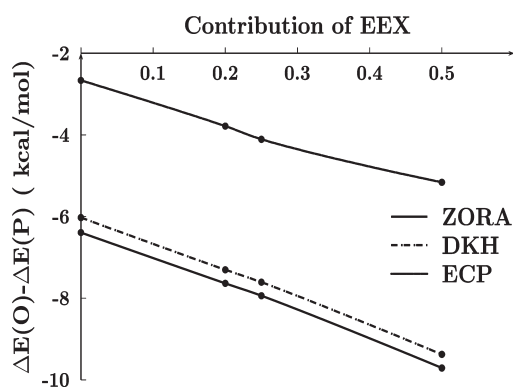


Figure 16. The relative stabilization of **O** with respect to **P** due to relativistic corrections calculated with BLYP, B3-LYP, B1-LYP, and BHandHLYP density functionals.

to change the position of the global minimum. It appears that a little less than half of the scalar relativistic effects are recovered in the ECP calculations (Figure 16).

Interestingly, the relativistic effect on the relative stability of the two isomers also strongly depends on the functional used. There appears to be a nearly linear correlation between the EEX contribution in the functional and the size of the relativistic corrections. This may well be related to the changes in metal–ligand covalency. With increasing EEX, the metal ligand bonds become more ionic. Thus, the d-electron count increases for both isomers with increasing EEX. As **O** has the lower formal

d-electron count, it is expected to be increasingly stabilized relative to **P** as EEX increases.

Compared to the value of 6.8 kcal/mol calculated at the CBS limit with ZORA, LPNO–CCSD after triples correction, the best result is delivered by BLYP-D which predicts an energy difference of 6.4 kcal/mol. B3LYP-D is also excellent and predicts a value of 7.6 kcal/mol.

Solvent Effects. The resulting COSMO corrected PESs are shown in Figure 17.

The results follow the same pattern already found on the LPNO–CCSD calculations thus favoring **O**. In quantitative terms, BLYP-D provides the best result and predicts a stabilization of 7.4 kcal/mol relative to the reference value of 6.4 kcal/mol. B3LYP-D is slightly worse and gives a value of 8.2 kcal/mol.

ORIGIN OF RELATIVISTIC EFFECTS

The origin of the significant relativistic effects is investigated by looking at the changes that occur in the molecular orbitals due to relativity. This is reasonable as the net relativistic effect is dominated by the changes in the SCF energy. The effects of scalar relativity on the B3LYP orbitals 42 up to 77 [the highest occupied molecular orbital (HOMO) is orbital 69] are investigated in Figure 18, where the energy difference of the individual orbitals with and without the ZORA correction is plotted.

The plot can be divided into four regions depending on which fragments dominate the molecular orbitals within a given region. The deeper occupied valence orbitals are mainly ligand in character (see Table S1 of the Supporting Information). As seen in the left of Figure 18, the relativistic effects on these orbitals are

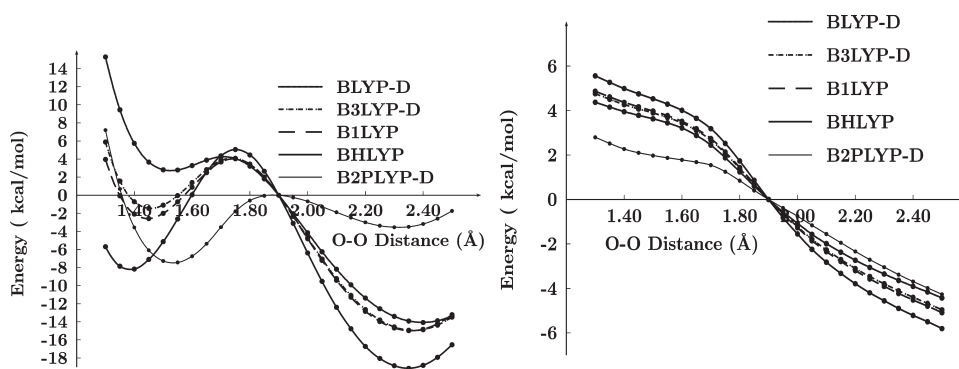


Figure 17. The potential energy using the density functional methods corrected for relativistic effects through ZORA, for dispersion forces through D and for solvent effects through COSMO, with CH_2Cl_2 solvent (left part). The effect of solvent (right part).

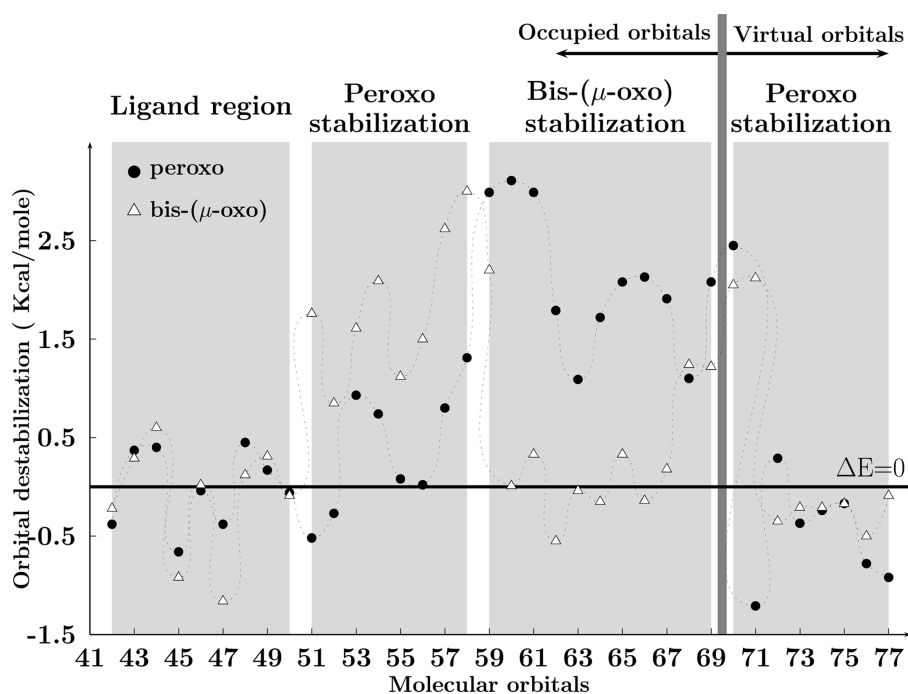


Figure 18. Changes in the B3LYP/def2-TZVP orbital energies due to ZORA for the two isomers. Orbitals are arbitrarily linked by wavy lines to facilitate visual comparison.

small and, more importantly, are almost identical for the two isomers. Hence these orbitals do not contribute to the preferential stabilization of **O** relative to **P**. Summed over all contributions in that region, a net 0.9 kcal/mol stabilization of **O** results which is probably within the noise.

The second region is defined by orbitals 51–58. Here one finds that the **P** orbitals are preferentially stabilized. Summed over all contributions results in a value of 11.5 kcal/mol. From Table S2 of the Supporting Information it becomes evident that in this region the strongly stabilized copper d-orbitals of **O** are located, while for **P** these orbitals are mainly of ligand s and p character. Since d-orbitals are stabilized by relativity, this region provides relativistic corrections in favor of **P**.

The opposite case is met in region 3, the upper valence region. Here copper d-orbitals dominate for **P**, while for **O** the highest occupied orbitals are mainly of ligand s and p character. Since the

latter are little affected by relativity, the sum over this region provides 18.4 kcal/mol relativistic effect in favor of **O**.

Thus the net relativistic effect can be traced back to the stronger destabilization of **P** relative to **O**. Summed over all molecular orbitals, a value of 7.8 kcal/mol in favor of **O** is obtained which is sufficiently close to the net relativistic stabilization energy of 5.3 kcal/mol. The preferential bias in favor of **O** is explained by the lower formal d-count (d^8 for **O** vs d^9 for **P**) and by the fact that **P** has less covalent metal ligand bonds and hence feels more of the d-orbital destabilization than **O**.

One final note concerns the effect in the lower lying unoccupied orbitals. In Figure 18 orbitals 70–77 have been included. It is apparent that **P** should be favored with respect to **O** as its orbitals are preferentially less destabilized than those of **O**. These decreased gaps between occupied and unoccupied orbitals will tend to increase the correlation energy. This may well explain the opposite trend for the correlation energies obtained in Figure 8.

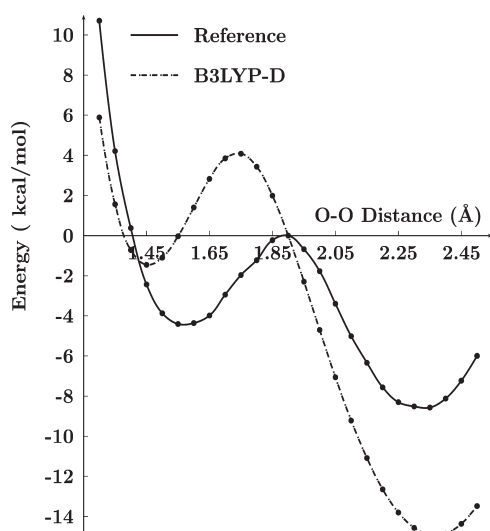


Figure 19. The most accurately calculated PES and the corresponding one calculated with B3LYP-D, ZORA and COSMO corrections using def2-TZVP basis set.

■ COMPARISON OF COUPLED CLUSTER AND DENSITY FUNCTIONAL CALCULATIONS

As reference curve, the scalar-relativistic CBS extrapolated LPNO–CCSD result together with solvent and triple-excitation corrections is used. Relative to this reference, the most accurate functional is B3LYP-D with a mean absolute error (MAE) of 4.4 kcal/mol, followed by B1LYP (4.5 kcal/mol) and BLYP-D (4.8 kcal/mol). In Figure 19 the reference PES is shown next to B3LYP-D. While the overall shape of the PES is correct with B3LYP-D, the quantitative performance is not quite satisfactory: The energy difference, between the two isomers, is overestimated with B3LYP by as much as 9.3 kcal/mol, and the position of the minimum for **P** is calculated to be 0.1 Å too short. Thus, none of the functionals can be considered as satisfactory if one gives preference to the wave function-based ab initio reference curve.

■ CONCLUSION

In this paper we have discussed some aspects of applying correlated wave function-based ab initio methods to transition-metal chemistry. To illustrate this subject, a fairly detailed study on the equilibrium between the bis-(μ -oxo) and peroxo isomers of $[\text{Cu}_2(\text{en})_2(\text{O})_2]^{2+}$ has been reported. A relaxed energy surface scan provided the reaction coordinate for the interconversion of the two isomers. Using the LPNO–CCSD method, the **O** isomer was found to be more stable than **P**, in agreement with the experimental results. The effect of relativity was found to be important, favoring the **O** isomer. This trend was consistent for the three different methods that were used to calculate the relativistic corrections, namely ZORA, DKH, and quasirelativistic ECP. The results for DKH and ZORA were almost identical. About half of the relativistic effect was obtained with ECPs. While this is somewhat displeasing, we note that ECPs also do not lead to dramatic computational savings over scalar relativistic all electron calculations. For this reason we prefer the latter. The effect of solvent (within the limits of the dielectric continuum model) was found to be significant as well and helps stabilizing **O** over **P** to an extent that mirrors the relativistic effect. Thus

theoretical studies neglecting these two contributions to the **O/P** equilibrium are grossly wrong.

Flock et al.³² in an early study on the **O–P** interconversion did include relativistic effects in their description but did not consider solvent effects. The same strategy was followed later by Rode and Werner⁹⁹ who included relativistic effects, though through the use of ECP's, but also left out solvent effects. Siegbahn in a very rigorous and detailed study⁷⁷ calculated the B3LYP energy difference between **O/P** and found it to be 8.3 kcal/mol. This result is in excellent agreement with the best ab initio results calculated in this work. However, the coincidentally perfect agreement is partly due to a cancellation of errors. Although all necessary corrections were considered, Siegbahn's calculations used the lacvp relativistic core potential. According to the calculations presented above, this implies that the stabilization of **O**, due to relativistic effects, is probably underestimated. In addition the lack of dispersion corrections also favors **P** relatively to **O**. Overall this would mean that some 4–5 kcal/mol of stabilization energy in favor of **O** should be added that would then lead to total stabilization close to 14 kcal/mol for **O**, which is in good agreement with our own B3LYP calculations. We note in passing that we agree with the comment of Cramer et al.,³¹ that larger ligands (as mostly used in actual chemical studies) will greatly reduce the importance of solvent corrections.

Five different functionals were compared to the LPNO–CCSD results (BLYP, B3LYP, B2LYP, BHandHLYP, and B2PLYP). With the exception of B2PLYP, they mainly differ in the percentage of exact exchange that is incorporated. In agreement with the literature,^{7,99} the addition of EEX systematically favors the **O** isomer with the stabilization being linearly proportional to the fractional EEX in the functional. The best agreement with the LPNO–CCSD results was obtained with the B3LYP functional once dispersion corrections were included. The double hybrid B2PLYP is not successful in this application because of the disastrous failure of MP2 for this system. However, none of the functionals can be considered to be in truly satisfactory agreement with the reference ab initio results. This clearly speaks in favor of continued efforts in the development of wave function-based ab initio results for applications in coordination and bioinorganic chemistry. The recent progress in the methodology is certainly encouraging in this respect.

■ ASSOCIATED CONTENT

S Supporting Information. The shape and composition of the molecular orbitals used for the analysis of the relativistic effects together with the Cartesian coordinates for all structures described. This material is available free of charge via the Internet at <http://pubs.acs.org/>.

■ AUTHOR INFORMATION

Corresponding Author

*E-mail: neese@thch.uni-bonn.de.

■ REFERENCES

- (1) Mahadevan, V.; Gebbink, R. J. M. K.; Stack, T. D. P. Biomimetic modeling of copper oxidase reactivity. *Curr. Opin. Chem. Biol.* **2000**, *4*, 228–234.
- (2) Sorrell, T. N. Synthetic models for binuclear copper proteins. *Tetrahedron* **1989**, *45*, 3–68.

- (3) Solomon, E.; Lowery, M. Electronic structure contributions to function in bioinorganic chemistry. *Science* **1993**, 259, 1575–1581.
- (4) L. Holland, P.; B. Tolman, W. Dioxygen activation by copper sites: relative stability and reactivity of (μ - η^2 : η^2 -peroxo)- and bis(μ -oxo) dicopper cores. *Coord. Chem. Rev.* **1999**, 190–192, 855–869.
- (5) Mirica, L. M.; Ottenwaelde, X.; Stack, T. D. P. Structure and Spectroscopy of Copper–Dioxygen Complexes. *Chem. Rev.* **2004**, 104, 1013–1046.
- (6) Lewis, E. A.; Tolman, W. B. Reactivity of Dioxygen–Copper Systems. *Chem. Rev.* **2004**, 104, 1047–1076.
- (7) Gherman, B. F.; Cramer, C. J. Quantum chemical studies of molecules incorporating a $\text{Cu}_2\text{O}_2^{2+}$ core. *Coord. Chem. Rev.* **2009**, 253, 723–753.
- (8) Solomon, E. I.; Sundaram, U. M.; Machonkin, T. E. Multicopper Oxidases and Oxygenases. *Chem. Rev.* **1996**, 96, 2563–2606.
- (9) Solomon, E. I.; Baldwin, M. J.; Lowery, M. D. Electronic structures of active sites in copper proteins: contributions to reactivity. *Chem. Rev.* **1992**, 92, 521–542.
- (10) Klinman, J. P. Mechanisms Whereby Mononuclear Copper Proteins Functionalize Organic Substrates. *Chem. Rev.* **1996**, 96, 2541–2562.
- (11) Schindler, S. Reactivity of Copper(I) Complexes Towards Dioxygen. *Eur. J. Inorg. Chem.* **2000**, 2000, 2311–2326.
- (12) Kitajima, N.; Moro-oka, Y. Copper-Dioxygen Complexes. Inorganic and Bioinorganic Perspectives. *Chem. Rev.* **1994**, 94, 737–757.
- (13) Solomon, E. I.; Tuzek, F.; Root, D. E.; Brown, C. A. Spectroscopy of Binuclear Dioxygen Complexes. *Chem. Rev.* **1994**, 94, 827–856.
- (14) Cole, A. P.; Mahadevan, V.; Mirica, L. M.; Ottenwaelde, X.; Stack, T. D. P. Bis(μ -oxo)dicopper(III) Complexes of a Homologous Series of Simple Peralkylated 1,2-Diamines: Steric Modulation of Structure, Stability, and Reactivity. *Inorg. Chem.* **2005**, 44, 7345–7364.
- (15) Land, E. J.; Ramsden, C. A.; Riley, P. A. Tyrosinase Autoactivation and the Chemistry of ortho-Quinone Amines. *Acc. Chem. Res.* **2003**, 36, 300–308.
- (16) Karlin, K. Metalloenzymes, structural motifs, and inorganic models. *Science* **1993**, 261, 701–708.
- (17) Holm, R. H.; Kennepohl, P.; Solomon, E. I. Structural and Functional Aspects of Metal Sites in Biology. *Chem. Rev.* **1996**, 96, 2239–2314.
- (18) Kitajima, N.; Fujisawa, K.; Fujimoto, C.; Morooka, Y.; Hashimoto, S.; Kitagawa, T.; Toriumi, K.; Tatsumi, K.; Nakamura, A. A new model for dioxygen binding in hemocyanin. Synthesis, characterization, and molecular structure of the μ - η^2 : η^2 -peroxo dinuclear copper(II) complexes, $[\text{Cu}(\text{HB}(3,5\text{-R}_2\text{pz})_3)_2(\text{O}_2)]$ (R = isopropyl and Ph). *J. Am. Chem. Soc.* **1992**, 114, 1277–1291.
- (19) Koder, M.; Katayama, K.; Tachi, Y.; Kano, K.; Hirota, S.; Fujinami, S.; Suzuki, M. Crystal Structure and Reversible O₂-Binding of a Room Temperature Stable μ - η^2 : η^2 -Peroxydicopper(II) Complex of a Sterically Hindered Hexapyridine Dinucleating Ligand. *J. Am. Chem. Soc.* **1999**, 121, 11006–11007.
- (20) Magnus, K. A.; Ton-That, H.; Carpenter, J. E. Recent Structural Work on the Oxygen Transport Protein Hemocyanin. *Chem. Rev.* **1994**, 94, 727–735.
- (21) Gamez, P.; Koval, I. A.; Reedijk, J. Bio-mimicking galactose oxidase and hemocyanin, two dioxygen-processing copper proteins. *Dalton Trans.* **2004**, 4079–4088.
- (22) Takano, Y.; Yamaguchi, K. Hybrid density functional study of ligand coordination effects on the magnetic couplings and the dioxygen binding of the models of hemocyanin. *Int. J. Quantum Chem.* **2007**, 107, 3103–3119.
- (23) Halfen, J. A.; Mahapatra, S.; Wilkinson, E. C.; Kaderli, S.; Young, V. G., Jr.; Que, L., Jr.; Zuberbühler, A. D.; Tolman, W. B. Reversible Cleavage and Formation of the Dioxygen O—O Bond Within a Dicopper Complex. *Science* **1996**, 271, 1397–1400.
- (24) Mahapatra, S.; Halfen, J. A.; Wilkinson, E. C.; Pan, G.; Wang, X.; Young, V. G.; Cramer, C. J.; Que, L.; Tolman, W. B. Structural, Spectroscopic, and Theoretical Characterization of Bis(μ -oxo)dicopper Complexes, Novel Intermediates in Copper-Mediated Dioxygen Activation. *J. Am. Chem. Soc.* **1996**, 118, 11555–11574.
- (25) DuBois, J. L.; Mukherjee, P.; Collier, A. M.; Mayer, J. M.; Solomon, E. I.; Hedman, B.; Stack, T. D. P.; Hodgson, K. O. Cu K-Edge XAS Study of the $[\text{Cu}_2(\mu\text{-O})_2]$ Core: Direct Experimental Evidence for the Presence of Cu(III). *J. Am. Chem. Soc.* **1997**, 119, 8578–8579.
- (26) Tyeklar, Z.; Jacobson, R. R.; Wei, N.; Murthy, N. N.; Zubieta, J.; Karlin, K. D. Reversible reaction of dioxygen (and carbon monoxide) with a copper(I) complex. X-ray structures of relevant mononuclear Cu(I) precursor adducts and the trans-(μ -1,2-peroxo)dicopper(II) product. *J. Am. Chem. Soc.* **1993**, 115, 2677–2689.
- (27) Jacobson, R. R.; Tyeklar, Z.; Farooq, A.; Karlin, K. D.; Liu, S.; Zubieta, J. A copper-oxygen ($\text{Cu}_2\text{-O}_2$) complex. Crystal structure and characterization of a reversible dioxygen binding system. *J. Am. Chem. Soc.* **1988**, 110, 3690–3692.
- (28) Kitajima, N.; Fujisawa, K.; Morooka, Y.; Toriumi, K. μ - η^2 : η^2 -Peroxy binuclear copper complex, $[\text{Cu}(\text{HB}(3,5\text{-Me}_2\text{CH})_2\text{pz})_3]_2(\text{O}_2)$. *J. Am. Chem. Soc.* **1989**, 111, 8975–8976.
- (29) Cramer, C. J.; Kinal, A.; Wloch, M.; Piecuch, P.; Gagliardi, L. Theoretical Characterization of End-On and Side-On Peroxide Coordination in Ligated Cu_2O_2 Models. *J. Phys. Chem. A* **2006**, 110, 11557–11568.
- (30) Cramer, C. J.; Smith, B. A.; Tolman, W. B. Ab Initio Characterization of the Isomerism between the μ - η^2 : η^2 -Peroxy- and Bis(μ -oxo)dicopper Cores. *J. Am. Chem. Soc.* **1996**, 118, 11283–11287.
- (31) Cramer, C. J.; Wloch, M.; Piecuch, P.; Puzzarini, C.; Gagliardi, L. Theoretical Models on the Cu_2O_2 Torture Track: Mechanistic Implications for Oxytyrosinase and Small-Molecule Analogues. *J. Phys. Chem. A* **2006**, 110, 1991–2004.
- (32) Flock, M.; Pierloot, K. Theoretical Study of the Interconversion of O₂-Binding Dicopper Complexes. *J. Phys. Chem. A* **1998**, 103, 95–102.
- (33) Malmqvist, P. A.; Pierloot, K.; Shahi, A. R. M.; Cramer, C. J.; Gagliardi, L. The restricted active space followed by second-order perturbation theory method: Theory and application to the study of CuO_2 and Cu_2O_2 systems. *J. Chem. Phys.* **2008**, 128, 204109–10.
- (34) Yanai, T.; Kurashige, Y.; Neuscamman, E.; Chan, G. K.-L. Multireference quantum chemistry through a joint density matrix renormalization group and canonical transformation theory. *J. Chem. Phys.* **2010**, 132, 024105–9.
- (35) Kowalski, K.; Piecuch, P. The method of moments of coupled-cluster equations and the renormalized CCSD[T], CCSD(T), CCSD-(TQ), and CCSDT(Q) approaches. *J. Chem. Phys.* **2000**, 113, 18–35.
- (36) Piecuch, P.; Kowalski, K.; Pimental, I. S. O.; Fan, P. D.; Lodriguito, M.; McGuire, M. J.; Kucharski, S. A.; Kuś, T.; Musiał, M. Method of moments of coupled-cluster equations: a new formalism for designing accurate electronic structure methods for ground and excited states. *Theor. Chem. Acc.* **2004**, 112, 349–393.
- (37) Piecuch, P.; Wloch, M.; Gour, J. R.; Kinal, A. Single-reference, size-extensive, non-iterative coupled-cluster approaches to bond breaking and biradicals. *Chem. Phys. Lett.* **2006**, 418, 467–474.
- (38) Saito, T.; Kataoka, Y.; Nakanishi, Y.; Matsui, T.; Kitagawa, Y.; Kawakami, T.; Okumura, M.; Yamaguchi, K. Theoretical studies on chemical bonding between Cu(II) and oxygen molecule in type 3 copper proteins. *Int. J. Quantum Chem.* **2009**, 109, 3649–3658.
- (39) Op't Holt, B. T.; Vance, M. A.; Mirica, L. M.; Heppner, D. E.; Stack, T. D. P.; Solomon, E. I. Reaction Coordinate of a Functional Model of Tyrosinase: Spectroscopic and Computational Characterization. *J. Am. Chem. Soc.* **2009**, 131, 6421–6438.
- (40) Kong, L.; Nooijen, M. Study of energetics of end-on and side-on peroxide coordination in ligated Cu_2O_2 models with State-Specific Equation of Motion Coupled Cluster Method. *Int. J. Quantum Chem.* **2008**, 108, 2097–2107.
- (41) Kurashige, Y.; Yanai, T. High-performance ab initio density matrix renormalization group method: Applicability to large-scale multi-reference problems for metal compounds. *J. Chem. Phys.* **2009**, 130, 234114.

- (42) Maddaluno, J.; Giessner-Prettre, C. Nonempirical calculations on dicopper(1+)-dioxygen: a possible model for oxyhemocyanin and oxytyrosinase active sites. *Inorg. Chem.* **1991**, *30*, 3439–3445.
- (43) Bernardi, F.; Bottoni, A.; Casadio, R.; Fariselli, P.; Rigo, A. An ab initio study of the dioxygen binding site of hemocyanin: A comparison between CASSCF, CASPT2, and DFT approaches. *Int. J. Quantum Chem.* **1996**, *58*, 109–119.
- (44) Siegbahn, P. E. M.; Wirstam, M. Is the Bis- μ -Oxo Cu₂(III,III) State an Intermediate in Tyrosinase? *J. Am. Chem. Soc.* **2001**, *123*, 11819–11820.
- (45) Aboelella, N. W.; Gherman, B. F.; Hill, L. M. R.; York, J. T.; Holm, N.; Young, V. G.; Cramer, C. J.; Tolman, W. B. Effects of Thioether Substituents on the O₂ Reactivity of β -Diketiminato-Cu(I) Complexes: Probing the Role of the Methionine Ligand in Copper Monooxygenases. *J. Am. Chem. Soc.* **2006**, *128*, 3445–3458.
- (46) Berces, A. Ligand Effects in the Models and Mimics of Oxyhemocyanin and Oxytyrosinase. A Density Functional Study of Reversible Dioxygen Binding and Reversible O—O Bond Cleavage. *Inorg. Chem.* **1997**, *36*, 4831–4837.
- (47) Berces, A. Density functional calculations of dioxygen binding in mono- and dinuclear copper complexes. *Int. J. Quantum Chem.* **1997**, *65*, 1077–1086.
- (48) Lam, B. M. T.; Halfen, J. A.; Young, V. G.; Hagadorn, J. R.; Holland, P. L.; Lledos, A.; Cucurull-Sanchez, L.; Novoa, J. J.; Alvarez, S.; Tolman, W. B. Ligand Macrocyclic Structural Effects on Copper-Dioxygen Reactivity. *Inorg. Chem.* **2000**, *39*, 4059–4072.
- (49) Liu, X.-Y.; Palacios, A. A.; Novoa, J. J.; Alvarez, S. Framework Bonding and Coordination Sphere Rearrangement in the M₂ × 2 Cores of Synthetic Analogues of Oxyhemocyanin and Related Cu and Pt Complexes. *Inorg. Chem.* **1998**, *37*, 1202–1212.
- (50) Metz, M.; Solomon, E. I. Dioxygen Binding to Deoxyhemocyanin: Electronic Structure and Mechanism of the Spin-Forbidden Two-Electron Reduction of O₂. *J. Am. Chem. Soc.* **2001**, *123*, 4938–4950.
- (51) Mirica, L. M.; Rudd, D. J.; Vance, M. A.; Solomon, E. I.; Hodgson, K. O.; Hedman, B.; Stack, T. D. P. μ - η^2 : η^2 -Peroxo-dicopper(II) Complex with a Secondary Diamine Ligand: A Functional Model of Tyrosinase. *J. Am. Chem. Soc.* **2006**, *128*, 2654–2665.
- (52) Siegbahn, P. E. M. Modeling aspects of mechanisms for reactions catalyzed by metalloenzymes. *J. Comput. Chem.* **2001**, *22*, 1634–1645.
- (53) Roos, B. O. *The Complete Active Space Self-Consistent Field Method and its Applications in Electronic Structure Calculations*; John Wiley & Sons, Inc.: Hoboken, NJ, 2007; pp 399–445.
- (54) Roos, B. O.; Taylor, P. R.; Siegbahn, P. E. M. A complete active space SCF method (CASSCF) using a density matrix formulated super-CI approach. *Chem. Phys.* **1980**, *48*, 157–173.
- (55) Andersson, K.; Malmqvist, P. A.; Roos, B. O.; Sadlej, A. J.; Wolinski, K. Second-order perturbation theory with a CASSCF reference function. *J. Phys. Chem.* **1990**, *94*, 5483–5488.
- (56) Neese, F.; Wennmohs, F.; Hansen, A. Efficient and accurate local approximations to coupled-electron pair approaches: An attempt to revive the pair natural orbital method. *J. Chem. Phys.* **2009**, *130*, 114108–18.
- (57) Neese, F.; Hansen, A.; Liakos, D. G. Efficient and accurate approximations to the local coupled cluster singles doubles method using a truncated pair natural orbital basis. *J. Chem. Phys.* **2009**, *131*, 064103–15.
- (58) Liakos, D. G.; Hansen, A.; Neese, F. Weak Molecular Interactions Studied with Parallel Implementations of the Local Pair Natural Orbital Coupled Pair and Coupled Cluster Methods. *J. Chem. Theory Comput.* **2010**, *7*, 76–87.
- (59) Mahadevan, V.; Henson, M. J.; Solomon, E. I.; Stack, T. D. P. Differential Reactivity between Interconvertible Side-On Peroxo and Bis- μ -oxodicopper Isomers Using Peralkylated Diamine Ligands. *J. Am. Chem. Soc.* **2000**, *122*, 10249–10250.
- (60) Mirica, L. M.; Vance, M.; Rudd, D. J.; Hedman, B.; Hodgson, K. O.; Solomon, E. I.; Stack, T. D. P. Tyrosinase Reactivity in a Model Complex: An Alternative Hydroxylation Mechanism. *Science* **2005**, *308*, 1890–1892.
- (61) Neese, F.; Becker, U.; Ganyushin, D.; Hansen, A.; Liakos, D. G.; Kollmar, C.; Kossmann, S.; Petrenko, T.; Reimann, C.; Riplinger, C.; Sivalingam, K.; Valeev, E.; Wezislá, B.; Wennmohs, F. ORCA; University of Bonn: Bonn, Germany, 2009.
- (62) Perdew, J. P.; Burke, K.; Ernzerhof, M. Generalized Gradient Approximation Made Simple. *Phys. Rev. Lett.* **1996**, *77*, 3865.
- (63) Grimme, S.; Antony, J.; Ehrlich, S.; Krieg, H. A consistent and accurate ab initio parametrization of density functional dispersion correction (DFT-D) for the 94 elements H–Pu. *J. Chem. Phys.* **2010**, *132*, 154104–19.
- (64) Schafer, A.; Horn, H.; Ahlrichs, R. Fully optimized contracted Gaussian basis sets for atoms Li to Kr. *J. Chem. Phys.* **1992**, *97*, 2571–2577.
- (65) Weigend, F.; Ahlrichs, R. Balanced basis sets of split valence, triple zeta valence and quadruple zeta valence quality for H to Rn: Design and assessment of accuracy. *Phys. Chem. Chem. Phys.* **2005**, *7*, 3297–3305.
- (66) Weigend, F.; Furche, F.; Ahlrichs, R. Gaussian basis sets of quadruple zeta valence quality for atoms H–Kr. *J. Chem. Phys.* **2003**, *119*, 12753–12762.
- (67) Feyereisen, M.; Fitzgerald, G.; Komornicki, A. Use of approximate integrals in ab initio theory. An application in MP2 energy calculations. *Chem. Phys. Lett.* **1993**, *208*, 359–363.
- (68) Kendall, R. A.; Früchtl, H. A. The impact of the resolution of the identity approximate integral method on modern ab initio algorithm development. *Theor. Chem. Acc.* **1997**, *97*, 158–163.
- (69) Lee, T. J.; Rendell, A. P.; Taylor, P. R. Comparison of the quadratic configuration interaction and coupled-cluster approaches to electron correlation including the effect of triple excitations. *J. Phys. Chem.* **1990**, *94*, 5463–5468.
- (70) Pople, J. A.; Head-Gordon, M.; Raghavachari, K. Quadratic configuration interaction. A general technique for determining electron correlation energies. *J. Chem. Phys.* **1987**, *87*, 5968–5975.
- (71) Becke, A. D. Density-Functional Exchange-Energy Approximation with Correct Asymptotic-Behavior. *Phys. Rev. A* **1988**, *38*, 3098–3100.
- (72) Lee, C. T.; Yang, W. T.; Parr, R. G. Development of the Colle-Salvetti Correlation-Energy Formula into a Functional of the Electron-Density. *Phys. Rev. B* **1988**, *37*, 785–789.
- (73) Becke, A. D. Density-Functional Thermochemistry 0.3. The Role of Exact Exchange. *J. Chem. Phys.* **1993**, *98*, 5648–5652.
- (74) Adamo, C.; Matteo, A. d.; Barone, V. From Classical Density Functionals to Adiabatic Connection Methods. the State of the Art. In *Advances in Quantum Chemistry*; P.-O. Löwdin, Sabin, J. R., Zerner, M. C., Brandas, E., Lami, A., Vincenzo, B., Eds.; Academic Press: San Diego, CA, 1999; Vol. 36, pp 45–75.
- (75) Becke, A. D. A new mixing of Hartree–Fock and local density-functional theories. *J. Chem. Phys.* **1993**, *98*, 1372–1377.
- (76) Grimme, S. Semiempirical hybrid density functional with perturbative second-order correlation. *J. Chem. Phys.* **2006**, *124*, 034108–16.
- (77) Siegbahn, P. E. M. A comparison of the thermodynamics of O—O bond cleavage for dicopper complexes in enzymes and synthetic systems. *J. Biol. Inorg. Chem.* **2003**, *8*, 577–585.
- (78) Hess, B. A. Relativistic electronic-structure calculations employing a two-component no-pair formalism with external-field projection operators. *Phys. Rev. A* **1986**, *33*, 3742.
- (79) Hess, B. A.; Marian, C. M. *Computational Molecular Spectroscopy*; Jensen, P., Bunker, P. R., Eds.; Wiley: New York, 2000 pp 169.
- (80) Jansen, G.; Hess, B. A. Revision of the Douglas-Kroll transformation. *Phys. Rev. A* **1989**, *39*, 6016.
- (81) Wolf, A.; Reiher, M.; Hess, B. A. *Relativistic Quantum Chemistry, Theoretical and Computational Chemistry*; Schwerdtfeger, P., Ed.; Elsevier: Amsterdam, The Netherlands, 2002; Vol. 1, pp 622.
- (82) Wolf, A.; Reiher, M.; Hess, B. A. *Recent Advances in Relativistic Molecular Theory*; Hirao, K.; Ishikawa, Y., Eds.; World Scientific: Singapore, 2004 pp 137.

- (83) van Lenthe, E.; Baerends, E. J.; Snijders, J. G. Relativistic regular two-component Hamiltonians. *J. Chem. Phys.* **1993**, *99*, 4597–4610.
- (84) van Lenthe, E.; Snijders, J. G.; Baerends, E. J. The zero-order regular approximation for relativistic effects: The effect of spin-orbit coupling in closed shell molecules. *J. Chem. Phys.* **1996**, *105*, 6505–6516.
- (85) Dolg, M.; Wedig, U.; Stoll, H.; Preuss, H. Energy-adjusted ab initio pseudopotentials for the first row transition elements. *J. Chem. Phys.* **1987**, *86*, 866–872.
- (86) Martin, J. M. L.; Sundermann, A. Correlation consistent valence basis sets for use with the Stuttgart–Dresden–Bonn relativistic effective core potentials: The atoms Ga–Kr and In–Xe. *J. Chem. Phys.* **2001**, *114*, 3408–3420.
- (87) Pantazis, D. A.; Chen, X.-Y.; Landis, C. R.; Neese, F. All-Electron Scalar Relativistic Basis Sets for Third-Row Transition Metal Atoms. *J. Chem. Theory Comput.* **2008**, *4*, 908–919.
- (88) Klamt, A.; Schuurmann, G. COSMO: a new approach to dielectric screening in solvents with explicit expressions for the screening energy and its gradient. *J. Chem. Soc., Perkin Trans. 2* **1993**, 799–805.
- (89) Tomasi, J. Thirty years of continuum solvation chemistry: a review, and prospects for the near future. *Theor. Chem. Acc.* **2004**, *112*, 184–203.
- (90) Tomasi, J.; Persico, M. Molecular Interactions in Solution: An Overview of Methods Based on Continuous Distributions of the Solvent. *Chem. Rev.* **1994**, *94*, 2027–2094.
- (91) Cramer, C. J.; Truhlar, D. G. Implicit Solvation Models: Equilibria, Structure, Spectra, and Dynamics. *Chem. Rev.* **1999**, *99*, 2161–2200.
- (92) Sinnecker, S.; Rajendran, A.; Klamt, A.; Diedenhofen, M.; Neese, F. Calculation of Solvent Shifts on Electronic σ -Tensors with the Conductor-Like Screening Model (COSMO) and Its Self-Consistent Generalization to Real Solvents (Direct COSMO-RS). *J. Phys. Chem. A* **2006**, *110*, 2235–2245.
- (93) Lee, T. J.; Taylor, P. R. A diagnostic for determining the quality of single-reference electron correlation methods. *Int. J. Quantum Chem.* **1989**, *36*, 199–207.
- (94) Neese, F. Prediction of molecular properties and molecular spectroscopy with density functional theory: From fundamental theory to exchange-coupling. *Coord. Chem. Rev.* **2009**, *253*, 526–563.
- (95) Helgaker, T.; Klopper, W.; Koch, H.; Noga, J. Basis-set convergence of correlated calculations on water. *J. Chem. Phys.* **1997**, *106*, 9639–9646.
- (96) Truhlar, D. G. Basis-set extrapolation. *Chem. Phys. Lett.* **1998**, *294*, 45–48.
- (97) Neese, F.; Valeev, E. F. Revisiting the Atomic Natural Orbital Approach for Basis Sets: Robust Systematic Basis Sets for Explicitly Correlated and Conventional Correlated ab initio Methods? *J. Chem. Theory Comput.* **2010**, *7*, 33–43.
- (98) Cramer, C. J. *Essentials of Computational Chemistry*, 2nd ed.; Wiley: New York, 2004; pp 179.
- (99) Rode, M. F.; Werner, H.-J. Ab initio study of the O₂ binding in dicopper complexes. *Theor. Chem. Acc.* **2005**, *114*, 309–317.
- (100) Huenerbein, R.; Schirmer, B.; Moellmann, J.; Grimme, S. Effects of London dispersion on the isomerization reactions of large organic molecules: a density functional benchmark study. *Phys. Chem. Chem. Phys.* **2010**, *12*, 6940–6948.
- (101) Goerigk, L.; Grimme, S. A General Database for Main Group Thermochemistry, Kinetics, and Noncovalent Interactions, ài Assessment of Common and Reparameterized (meta-)GGA Density Functionals. *J. Chem. Theory Comput.* **2009**, *6*, 107–126.
- (102) van Wullen, C. Molecular density functional calculations in the regular relativistic approximation: Method, application to coinage metal diatomics, hydrides, fluorides and chlorides, and comparison with first-order relativistic calculations. *J. Chem. Phys.* **1998**, *109*, 392–399.